INSTITUTE OF PHYSICS PUBLISHING EUROPEAN JOURNAL OF PHYSICS

Eur. J. Phys. **26** (2005) S47–S55 doi:10.1088/0143-0807/26/5/S06

Phase-field models for free-boundary problems

Thierry Biben

Laboratoire de Spectrométrie Physique, Université Joseph Fourier Grenoble I and CNRS (UMR5588), 140 avenue de la physique, BP87, 38 402 Saint Martin d'Hères Cedex, France

Received 23 May 2005
Published 4 July 2005
Online at stacks.iop.org/EJP/26/S47

Abstract

Phase-field models are very attractive in view of their numerical simplicity. With only a few lines of code, one can model complex physical situations such as dendritic growth. From this point of view, they constitute very interesting tools for teaching purposes at graduate level. The main difficulty with these models is in their formulation, which incorporates the physical ingredients in a subtle way. We discuss these approaches on the basis of two examples: dendritic growth and multiphase flows.

(Some figures in this article are in colour only in the electronic version)

1. Introduction

Phase-field (PF) models were proposed 20 years ago to tackle the difficult problem of crystal growth. From the original work by Collins and Levine [1] for the simulation of diffusion-limited crystal growth, the PF approach has been extended to dendritic growth by Kobayashi [2], and later by Karma and Rappel [3], and to stress-induced instabilities in solids by Kassner and Misbah [4]. The main idea behind PF models is to replace the singular macroscopic treatment of an interface (a discontinuity surface) by a regularized description. To this end, an auxiliary field varying smoothly across the interface is introduced: the PF. The original sharp interface formulation is thus rewritten to account for a smooth interface, and a supplementary evolution equation for the PF is added. The complexity induced by the singularities in the sharp interface description simply disappears in the PF formulation since there is, strictly speaking, no more interface. However, the PF equation contains its own physical ingredients that can serve or plague the model.

Although originally restricted to the domain of solid-state physics, these models have recently been adapted by several groups to address a large variety of domains. In fluid mechanics, Hele–Shaw instabilities [5], Marangoni convection [6], droplet and vesicle dynamics [7–10] and polymer blends [11] are examples of applications of these models. PF models are at the moment a very active research field since they only require a moderate computational effort. In view of their conceptual and computational simplicity, they constitute

a very attractive tool for teaching purposes and allow a student not familiar with complex domain decomposition methods to write a simple code able to reproduce phenomena as complex as dendritic growth or viscous fingering. Moreover, since most PF models are based on the same Landau–Ginzburg description of binary interfaces, only slight modifications are necessary to convert a crystal growth program into a model for Hele–Shaw flows, for example. These two properties, flexibility and simplicity, are at the origin of the growing popularity of these models.

We may, however, wonder why after 20 years these models are still research tools. The point is that PF models are 'models'; they do not yet constitute a 'method'. The main difficulty with these models is indeed in their formulation, not in the numerical implementation. Although these models share the same Landau–Ginzburg approach, the differences between them are often hidden in subtle coupling or counter-terms. There is thus no unified framework at the moment allowing us to define a PF method. In contrast, PF models need to be manipulated with a lot of caution, but from this point of view they constitute a subtle and fascinating toolbox for manipulating physics without much computational effort, and should thus become widely used for teaching purposes in the future.

We shall not make an exhaustive review of all the models suggested in the literature; we refer the readers to the references already mentioned for various examples. We discuss in the next few sections two elementary examples: Kobayashi's model for dendritic growth as an example of an 'active PF model', and an attempt suggested recently in fluid mechanics to formulate a generic 'passive PF model' (or advected field model), a potential first step towards a PF method.

But before considering these two examples, let us first discuss briefly the Landau–Ginzburg theory of binary interfaces.

2. The Landau–Ginzburg model

We shall discuss in this part the basic properties of the Landau–Ginzburg description of binary systems. This formulation is indeed the cornerstone of PF models, but contains physical ingredients that might or might not be desirable for the system under investigation, such as surface tension. We refer the reader to [12] for a more complete discussion.

The basic role of the PF 'θ' is to identify the coexisting phases. Since we consider here homogeneous and isotropic bulk phases, θ is simply a scalar field. More complex prescriptions can account for anisotropic phases if necessary, as in liquid crystals or magnetic systems for which orientational ordering is crucial. We can arbitrarily choose $\theta = \pm 1$ for the coexisting bulk phases. Any intermediate value shall indicate the proximity of an interface in the following. Such a phase coexistence is easily obtained by minimization of the bulk free energy

$$W(\theta) = (1 - \theta^2)^2/4. \tag{1}$$

This function has indeed two minima corresponding to $W = 0$ in $\theta = \pm 1$ (see figure 1). If we consider now a spatially inhomogeneous situation and simply replace θ by $\theta(\mathbf{r})$, where $\mathbf{r}$ indicates the position, integration of (1) over the whole space leads to the so-called local density approximation (LDA). This approximation is unfortunately too simplistic to describe an interface with a finite width since any spatial configuration with $\theta(\mathbf{r}) = \pm 1$ is a minimum. There is no energy cost for a spatial variation of $\theta(\mathbf{r})$ (and thus no surface tension). This problem can be solved by adding a gradient contribution

$$\mathcal{F}[\theta] = \int \mathrm{d}\mathbf{r} \left\{ W(\theta(\mathbf{r})) + \epsilon^2 \frac{[\nabla\theta(\mathbf{r})]^2}{2} \right\}. \tag{2}$$

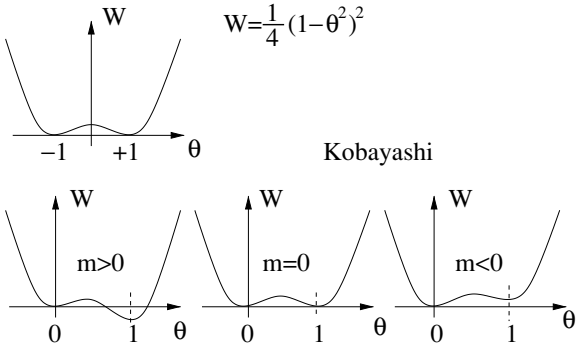

Figure 1. Schematic view of the Landau–Ginzburg free-energy functions. The top graph represents the function used for multiphase flows while the bottom graphs correspond to Kobayashi's prescription for dendritic growth.

The gradient appears in this expression through its modulus since the precise orientation of the interface is not important. We shall refer to this formulation as the 'square-gradient' model. From a dimensional analysis, ϵ is a length scale. This parameter is, in fact, up to a multiplicative constant, the interfacial width. To quantify this more precisely, (2) can be minimized explicitly in a planar geometry (translational invariance in the x, y directions) with the boundary conditions $\theta(z = -\infty) = -1$ and $\theta(z = +\infty) = +1$. After some algebra, one finds

$$\theta(z) = \tanh(z/(\epsilon\sqrt{2})). \tag{3}$$

The interfacial width is thus identified as $\epsilon\sqrt{2}$. Since the square-gradient model penalizes the variations of the PF, the presence of an interface results in an excess of energy (surface tension σ). σ can be calculated for a planar interface by inserting the tanh profile (3) in (2) (more details will be found in [12]):

$$\sigma = \epsilon \int_{-1}^{+1} \sqrt{2W(\theta)}\, \mathrm{d}\theta. \tag{4}$$

This formulation has the advantage of emphasizing the proportionality of σ with respect to ϵ. We immediately see that in the 'sharp interface limit' ($\epsilon \to 0$), $\theta(z)$ goes to a step profile and σ vanishes, as expected, since we recover the LDA model.

We shall now come back to our original goal: to use a smooth interface description to solve a sharp interface problem. It is tempting to use the PF surface tension σ to account for surface energy effects in the sharp interface problem (active PF). From the previous analysis, such a formulation requires a careful analysis of the sharp interface limit to prevent these effects to vanish. In contrast, 'passive PF' formulations do not make use of σ. Surface energy effects are accounted for in a separate way. σ thus appears in these passive approaches as a side effect to compensate, if possible. We shall emphasize this point in the next few sections.

3. Dendritic growth: active phase field

We shall present here the model used by Kobayashi [2] to describe dendritic growth. These structures can appear when a fluid is under-cooled below its solidification point. Solidification can start at some point in the system (usually induced by the presence of impurities) resulting in the propagation of a solidification front. The propagation velocity depends essentially on

limiting phenomena such as thermal diffusion. Indeed, the growth of an ordered phase in a disordered phase relaxes heat and thus locally heats up the system. If heat is not evacuated from the interfacial region (the propagating front), the growth should stop simply because the local temperature goes above the solidification point. Kobayashi's model thus accounts both for thermal diffusion through a local temperature field $T(\mathbf{r}, t)$ and for the growth of the solid phase through the PF $\theta(\mathbf{r}, t)$. The basic equations to solve are

$$\tau \frac{\partial \theta}{\partial t} = -\frac{\delta F[\theta]}{\delta \theta}, \qquad \frac{\partial T}{\partial t} = \Delta T + K \frac{\partial \theta}{\partial t}, \tag{5}$$

where τ is the typical relaxation time of the PF, $F[\theta]$ is essentially the square-gradient free-energy functional presented above with a slightly different prescription for $W(\theta)$ (see figure 1) and also for ϵ as we shall discuss in the following. The second equation is simply the thermal diffusion in the system, with a source term accounting for heat relaxation at the interface (θ varies only in the interfacial region so that $\partial\theta/\partial t$ is non-zero only there). These equations are in dimensionless units so that the diffusion constant is unity and K is a dimensionless latent heat. The prescription chosen for $W(\theta)$ has to ensure the growth of the solid phase thus it is not possible to consider the simple prescription (1) since it corresponds to a phase equilibrium (the two minima are at the same level). Growth of one phase with respect to the other occurs when its free energy is lower thus it is necessary to introduce an asymmetry in the free-energy functional. Kobayashi considered a double-well free-energy functional with the two minima in $\theta = 0$ and $\theta = 1$ (and not $\theta = \pm 1$) of the form

$$W(\theta) = \frac{\theta^4}{4} - \left(\frac{1}{2} - \frac{m}{3}\right)\theta^3 + \left(\frac{1}{4} - \frac{m}{2}\right)\theta^2, \tag{6}$$

where m is a constant fixing the distance to equilibrium. $m > 0$ favours phase $\theta = 1$ whereas $m < 0$ favours $\theta = 0$ (figure 1). $m = 0$ is the phase equilibrium. The complicated coefficients in (6) are simply chosen to force the minima to be in $\theta = 0$ or 1, whatever the value of m. Since growth is driven by the difference between the actual temperature T and the solidification temperature T_e, one can adopt several prescriptions. We shall consider Kobayashi's prescription $m = \frac{\alpha}{\pi}\tan^{-1}(\gamma(T_e - T))$ in the following (α and γ are phenomenological parameters). It can seem surprising to use a scalar order parameter to describe a crystalline phase, where both positional and orientational ordering exist. θ can, in fact, be viewed as a macroscopic order parameter field (i.e. a coarse-grained description of the solid phase like, for example, the averaged density field). Such a description does not account for the anisotropic growth observed in nature (for example, in snow flakes). To introduce anisotropy, Kobayashi assumed an angular dependence of the interfacial width $\epsilon = \epsilon(\phi)$, where ϕ indicates the orientation of the interface with respect to an arbitrary direction. ϕ can be defined as the angle between $\nabla\theta$ and the 'x' axis in 2D, since this vector is normal to the interface. A modulation of the interfacial width is directly related to a modulation of the surface tension (4) and thus of the growth velocity. Following Kobayashi, we set $\epsilon(\phi) = \epsilon(1 + \delta \sin(a(\phi - \phi_0))$, where ϵ is the average interfacial width, δ is the modulation amplitude, a is the mode number of anisotropy (the hexagonal symmetry corresponds to $a = 6$) and ϕ_0 allows us to vary the axis directions. The final PF equations are in 2D:

$$\tau \frac{\partial \theta}{\partial t} = -\frac{\partial}{\partial x}\left(\epsilon\epsilon' \frac{\partial \theta}{\partial y}\right) + \frac{\partial}{\partial y}\left(\epsilon\epsilon' \frac{\partial \theta}{\partial x}\right) + \epsilon^2 \Delta\theta + \nabla(\epsilon^2)\cdot\nabla\theta + \theta(1-\theta)(\theta - 1/2 + m(T)),$$

$$\frac{\partial T}{\partial t} = \Delta T + K \frac{\partial \theta}{\partial t}. \tag{7}$$

Here, $\epsilon \equiv \epsilon(\phi)$ and $\epsilon' \equiv \mathrm{d}\epsilon(\phi)/\mathrm{d}\phi$. Although these equations in their final form look complicated, they can be very simply solved numerically with a few instructions, as can be

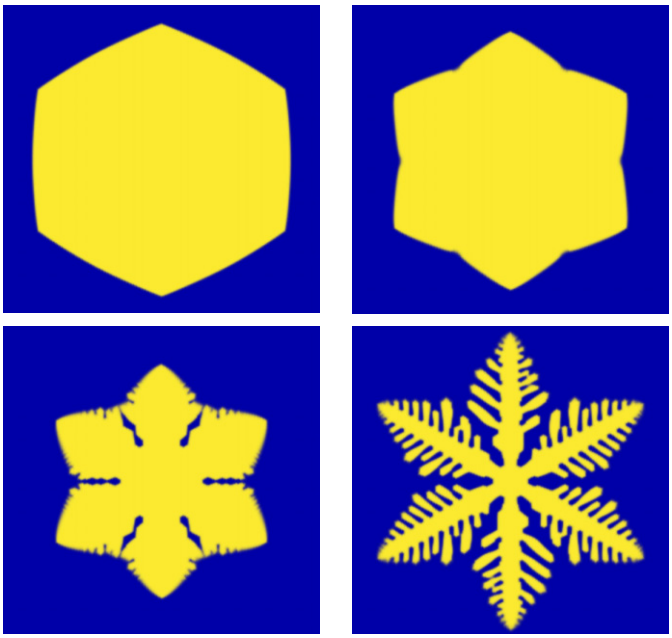

Figure 2. Different growth regimes as obtained from Kobayashi's model. The four images correspond to a dimensionless latent heat $K = 0.8, 1.0, 1.2$ and 1.8 from left to right and top to bottom; the dimensionless relaxation time is $\tau = 3 \times 10^{-4}$. The values of the more technical parameters are specified at the beginning of the 'C' program listed in the appendix.

seen in the 'C' program listed in the appendix. This simple code can be improved using more precise integration and derivation schemes, but this very basic implementation is indeed able to provide the data presented in figure 2. Although the main physical control parameter is the latent heat K, many auxiliary phenomenological parameters enter into play. An important effort has thus been devoted to the connexion between these parameters and physical quantities in later PF formulations.

4. Application to multiphase flows: passive phase field

This part illustrates how the Landau–Ginzburg approach can be used to derive a relatively generic PF formulation for free-boundary problems. Let us, for example, consider a multiphase flow where all the phases are simple Newtonian fluids. The dynamics of this system is given by the Navier–Stokes equation, in the presence of interfaces:

$$\rho\left(\frac{\partial \mathbf{v}}{\partial t} + \mathbf{v}\cdot\nabla\mathbf{v}\right) = \nabla\cdot(2\eta\mathbf{D}) - \nabla P + \mathbf{F}^{\text{int}}. \tag{8}$$

Here, ρ is the local mass density of the fluid, $\mathbf{v}$ is the velocity field, η is the local viscosity, $\mathbf{D}$ is the symmetric part of the velocity gradient tensor $\mathbf{D} = (\nabla\mathbf{v} + (\nabla\mathbf{v})^t)/2$, P is the local pressure field and $\mathbf{F}^{\text{int}}$ is the local force field applied by the interfaces to the flow. We assume the local incompressibility condition $\nabla\cdot\mathbf{v} = 0$. The main difficulty in solving numerically equation (8) is the singular nature of $\mathbf{F}^{\text{int}}$. This force field is indeed located at the interfaces and induces some discontinuities in the velocity gradient tensor. To solve this problem, one can solve the hydrodynamic equation in each phase separately, rejecting the force field $\mathbf{F}^{\text{int}}$

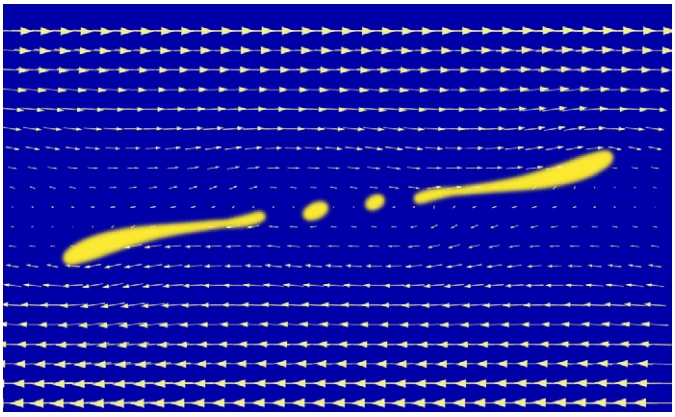

Figure 3. Break-up of a drop in a shear flow for a viscosity ratio $\eta_{\text{drop}}/\eta_{\text{solvent}} = 0.01$.

in the boundary conditions. The problem is two-fold: first, it is necessary to reconnect the resolution domains in a self-consistent way, and next, the boundaries are not fixed since they are transported by the flow. A mesh initially well adapted to a given configuration of the interfaces is likely to become very problematic after a few steps only, even worse is the coalescence of two domains (two drops, for example) where a complete re-meshing is usually necessary. The PF model solves these two problems by simply removing the singularities. At the microscopic level, an interface is not sharp and there are correlation lengths in a fluid below which a local (macroscopic) description is no longer valid. We can thus expect a model with smooth interfaces to describe in a better way the microscopic nature of the interfaces. The square-gradient model presented above is indeed able to account for topology changes in a continuous way: two drops are able to fuse or a drop can be broken without discontinuity since the PF can continuously go from -1 to $+1$ (see figure 3). In fact, the notion of domain topology itself has no real meaning without an additional prescription (for example, $\theta = 0$ is the locus of the interface separating the domains). This is the power of PF models. The main disadvantage is of course that the interfacial width is in reality very small (a few nanometres), leading to a value of $\epsilon \simeq 10^{-5}$, which is out of reach in practice. As a consequence, the PF methods are all plagued by an overestimated smoothness of the interfaces. This overestimation can have very strong consequences going from quantitative discrepancies to a wrong physics. On the other hand, the tremendous simplification obtained with these models compared to the original sharp interface formulation tends to generalize their usage. It is thus important to control the influence of ϵ on the results and to build models with fast convergence when $\epsilon \to 0$.

In the basic case of binary flows, a natural PF formulation could be written as

$$\rho(\theta)\left(\frac{\partial \mathbf{v}}{\partial t} + \mathbf{v}\cdot\nabla\mathbf{v}\right) = \nabla\cdot(2\eta(\theta)\mathbf{D}) - \nabla P + \mathbf{F}^{\text{int}}(\theta), \tag{9}$$

$$\frac{\partial \theta}{\partial t} + \mathbf{v}\cdot\nabla\theta = -\Gamma\frac{\delta \mathrm{F}}{\delta\theta}. \tag{10}$$

This formulation is unfortunately not satisfactory at non-vanishingly small values of ϵ (it overestimates diffusive transport, as discussed below), but a very simple modification suggested in [5] is sufficient to improve it in a substantial way. The Navier–Stokes equation as written in (9) only differs from (8) by the θ dependence of the physical parameters characterizing the bulk phases (η and ρ). For a binary system with two phases of viscosities η_1

and η_2, one can simply prescribe $\eta(\theta) = \eta_1\left(\frac{1+\theta}{2}\right) + \eta_2\left(\frac{1-\theta}{2}\right)$ (idem for ρ). $\theta = 1$ corresponds to phase 1 and $\theta = -1$ to phase 2. The force field $\mathbf{F}^{\text{int}}(\theta)$ is now a regular field centred on the interface but varying smoothly between 0 inside each phase to its interfacial value. The gradient of the PF as an indicator of the interface can be used:

$$\mathbf{F}^{\text{int}}(\theta) \equiv \mathbf{f}^{\text{int}}(\theta)\frac{|\nabla\theta|}{2}. \tag{11}$$

The prefactor $1/2$ ensures the normalization of $|\nabla\theta|/2$ across the interface (thanks to the variation of θ between -1 and $+1$). As an illustration, the force field corresponding to capillary forces can be written as

$$\mathbf{F}^{\text{int}} = \frac{c(\theta)}{2}\Sigma\nabla\theta,$$

where $c(\theta)$ is the local curvature field and Σ is the surface tension (not to be confused with σ introduced previously). c is related to θ through the normal unit vector field $\hat{\mathbf{n}} = \nabla\theta/|\nabla\theta|$ by $c(\theta) = -\nabla\cdot\hat{\mathbf{n}}$ (with this convention c is negative for a sphere). Since all the quantities entering in the Navier–Stokes equation (9) are smooth functions, this equation can be solved numerically on the whole simulation domain with the standard techniques. Both the interfaces and the boundary conditions associated with them are automatically accounted for by $\mathbf{F}^{\text{int}}(\theta)$.

The second equation (10) describes the dynamics of the PF and thus the dynamics of the interfaces. For the binary system we consider here, interfaces are simply transported by the flow. A transport equation for the PF of the type $\partial\theta/\partial t + \mathbf{v}\cdot\nabla\theta = 0$ (advection equation) does, however, not preserve the tanh profile across the interface, and does not ensure the phase equilibrium at rest. A restoring term is thus necessary as written in (10). Several prescriptions are possible: Γ is a simple constant fixing the relaxation time to the tanh profile, in which case we have an Allen–Cahn dynamics, or $\Gamma = -\Gamma'\Delta$, where Δ is a Laplacian operator acting on $\delta\mathrm{F}[\theta]/\delta\theta(\mathbf{r})$ and Γ' is a constant (Cahn–Hilliard dynamics). The second prescription ensures a conservation of the PF $\int\theta(\mathbf{r})\,\mathrm{d}\mathbf{r} = \text{cste}$ and is thus preferable here since we consider non-miscible fluids.

We now need to discuss the physics contained in this equation. Whereas the left-hand side of the PF equation (10) expresses the transport associated with the macroscopic velocity field, the right-hand side accounts for the relaxation of the interface in a diffusive way. This second effect has the consequence that even in the absence of macroscopic flow, a drop of arbitrary initial shape will relax to its stable spherical shape if the dynamics is conserved (Cahn–Hilliard) or even disappear if not. The relaxation time depends on the value of ϵ: in the sharp interface limit, the macroscopic situation, this time is infinite and the shape evolution of the interface is entirely driven by the macroscopic flow as expected. For a finite, numerically tractable, value of ϵ (i.e. $\epsilon \simeq 4\times10^{-2}$, instead of $\epsilon \simeq 10^{-5}$), this relaxation time is strongly overestimated and interferes with the advective dynamics. A solution is to cancel the first-order terms in ϵ appearing in the sharp interface limit of (10). This solution simply consists of adding the counter-term $\Gamma\epsilon^2 c\,|\nabla\theta|$ in (10) [5]. Using the explicit expression for the free-energy functional (2), the new equation is

$$\frac{\partial\theta}{\partial t} + \mathbf{v}\cdot\nabla\theta = -\Gamma\left\{\frac{\mathrm{d}W(\theta)}{\mathrm{d}\theta} - \epsilon^2(\Delta\theta + c\,|\nabla\theta|)\right\}. \tag{12}$$

The counter-term has the basic effect of compensating the surface tension σ of the square-gradient model at first order in ϵ. Mathematically, the counter-term reduces the Laplacian operator to $\Delta\theta + c\,|\nabla\theta| \simeq \partial^2\theta/\partial r^2 + \mathcal{O}(\epsilon^2)$ in the vicinity of the interface, r is the coordinate in the normal direction. We are thus no longer sensitive to the variations in the parallel direction. The PF profile remains $\theta(r) = \tanh(r/(\epsilon\sqrt{2}))$ across the interface whatever its local curvature, up to second order in ϵ. This new equation corresponds to a passive transport of the interface

```
// Phase-Field program, Dendritic growth using the model suggested by Kobayashi

#include <stdio.h>
#include <string.h>
#include <math.h>

#define     K       1.8         // Latent heat
#define     TAU     0.0003      // PF relaxation time

#define     EPS     0.01        // interfacial width
#define     DELTA   0.02        // modulation of the interfacial width
#define     ANGLE0  1.57        // orientation of the anisotropy axis
#define     ANISO   6.0         // anisotropy 2*PI/ANISO

#define     ALPHA   0.9         // m(T) = ALPHA/PI * atan(GAMMA*(TEQ-T))
#define     GAMMA   10.0
#define     TEQ     1.0         // melting temperature

#define     NX      300         // size of the mesh NX*NY
#define     NY      300
#define     H       0.03        // spatial resolution
#define     DT      2.e-4       // temporal resolution
#define     NTIME   2000        // number of time steps
#define     PI      3.14159265358

struct vec2D { double x, y;};

double get_angle( double x, double y )
{   double      angle;
    if (x==0.0)         angle = (y>0.0 ? 0.5*PI : -0.5*PI);
    else if (x>0.0)     angle = (y>0.0 ? atan(y/x) : 2.0*PI + atan(y/x));
    else                angle = PI + atan(y/x);
    return angle; };

main(int argc, char *argv[])
{   int             i, j, t, ip, im, jp, jm;
    double          theta[NX][NY], T[NX][NY], eps2[NX][NY], lap_T[NX][NY], lap_theta[NX][NY], m,
                    ax[NX][NY], ay[NX][NY], epsilon, epsilon_prime, angle, tet, dydx, dxdy, scal;
    struct vec2D    grad_theta[NX][NY], grad_eps2;
    FILE            *fp;
    char            file[100];

//  initial configuration: T=0 and theta=1 in a cercle of radius 3H (0 elsewhere).
    for(i=0;i<NX;i++) for(j=0;j<NY;j++) {T[i][j] = 0.0;
                                         theta[i][j] = ((i-NX/2)*(i-NX/2)+(j-NY/2)*(j-NY/2)<10)?1.0:0.0;}

//  temporal evolution
    for (t=0;t<NTIME;t++) {

        // computation of various auxiliary quantities
        for (i=0;i<NX;i++){ for (j=0;j<NY;j++){

            ip = (i+1)%NX;          // i+1 with Periodic Boundaries
            im = (NX+i-1)%NX;       // i-1 with Periodic Boundaries
            jp = (j+1)%NY;          // j+1 with Periodic Boundaries
            jm = (NY+j-1)%NY;       // j-1 with Periodic Boundaries

            // gradient and laplacians (order H^2, 9 points isotropic version for laplacians)
            grad_theta[i][j].x = (theta[ip][j] - theta[im][j])/H;
            grad_theta[i][j].y = (theta[i][jp] - theta[i][jm])/H;

            lap_theta[i][j] = (2.0*(theta[ip][j]+theta[im][j]+theta[i][jp]+theta[i][jm])
                 +theta[ip][jp]+theta[im][jm]+theta[im][jp]+theta[ip][jm] - 12.0*theta[i][j])/(3.0*H*H);
            lap_T[i][j] = (2.0*(T[ip][j]+T[im][j]+T[i][jp]+T[i][jm])
                 +T[ip][jp]+T[im][jm]+T[im][jp]+T[ip][jm] - 12.0*T[i][j])/(3.0*H*H);

            // angular dependence of the interfacial width "espilon"
            angle         = get_angle(grad_theta[i][j].x,grad_theta[i][j].y);
            epsilon       = EPS*(1.0 + DELTA*cos(ANISO*(angle-ANGLE0)));
            epsilon_prime = -EPS*ANISO*DELTA*sin(ANISO*(angle-ANGLE0));

            // auxiliary quantities appearing in the phase field equation
            ay[i][j]      = - epsilon*epsilon_prime * grad_theta[i][j].y;
            ax[i][j]      =   epsilon*epsilon_prime * grad_theta[i][j].x;
            eps2[i][j]    =   epsilon*epsilon;
        }}

        // simple Euler step
        for (i=0;i<NX;i++){ for (j=0;j<NY;j++){

            // first, some few spatial derivatives
            ip = (i+1)%NX;
            im = (NX+i-1)%NX;
            jp = (j+1)%NY;
            jm = (NY+j-1)%NY;

            dxdy = (ay[ip][j] - ay[im][j])/H;
            dydx = (ax[i][jp] - ax[i][jm])/H;
            grad_eps2.x  = (eps2[ip][j]  - eps2[im][j])/H;
            grad_eps2.y  = (eps2[i][jp]  - eps2[i][jm])/H;

            tet  = theta[i][j];
            m    = ALPHA/PI * atan(GAMMA*(TEQ-T[i][j]));
            scal= grad_eps2.x*grad_theta[i][j].x+ grad_eps2.y*grad_theta[i][j].y;

            // Euler step
            theta[i][j] += (dxdy+dydx + eps2[i][j]*lap_theta[i][j] + scal + tet*(1.0-tet)*(tet-0.5+m))*DT/TAU;
            T[i][j]     +=  lap_T[i][j]*DT + K*(theta[i][j] - tet);
        }}
    }

    // saving results
    sprintf(file,"theta.dat"); fp = fopen(file,"w");
    for (i=0;i<NX;i++) for (j=0;j<NY;j++) fprintf(fp," %d %d %e\n",i,j,theta[i][j]);
    fclose(fp);
    sprintf(file,"T.dat"); fp = fopen(file,"w");
    for (i=0;i<NX;i++) for (j=0;j<NY;j++) fprintf(fp," %d %d %e\n",i,j,T[i][j]);
    fclose(fp);
}
```

Figure A.1. Phase-Field program: dendritic growth using the model suggested by Kobayashi.

by the flow ('passive' PF). Equations (9) and (12) are the appropriate formulation for the description of binary fluids.

5. Conclusion

PF models provide a very flexible tool to solve in a simple numerical way complex free-boundary problems. The two examples chosen to illustrate this point show that complexity is still present, but now appears in the formulation of the model itself. It is thus interesting for teaching purposes to build the models starting from the simplest prescription for the PF equation (a simple relaxation equation, without any counter-term) and to add extra contributions very progressively, testing at each step the physical properties of each term.

Appendix

A.1. Numerical implementation of Kobayashi's model

From an initial solid nucleus located at the centre of the square resolution mesh of size $Nx \times Ny$ and lattice spacing h, equations (7) can be solved iteratively. Gradients are estimated using the simplest finite-difference formulation, while Laplacians require a nine-point isotropic finite-difference scheme to have reasonable accuracy. The boundary conditions at the edges of the mesh are chosen as periodic to limit finite-size effects both for the PF θ and the temperature field. The notation used in the code has been chosen to phonetically correspond to the quantities present in (7). A basic iteration step consists in estimating the various spatial derivatives involved in (7) from the knowledge of $T(\mathbf{r})$ and $\theta(\mathbf{r})$ at a given time t (the first loop on indices i and j—x and y coordinates—allows us to compute $\nabla\theta$, $\Delta\theta$, ΔT and the auxiliary quantities $\epsilon^2(\phi)$, $\epsilon\epsilon'\frac{\partial\theta}{\partial y}$ and $\epsilon\epsilon'\frac{\partial\theta}{\partial x}$ while $\nabla\epsilon^2$, $\frac{\partial}{\partial x}\left(\epsilon\epsilon'\frac{\partial\theta}{\partial y}\right)$ and $\frac{\partial}{\partial y}\left(\epsilon\epsilon'\frac{\partial\theta}{\partial x}\right)$ are estimated at the beginning of the second loop). From these values, the new temperature and phase field can be estimated at time $t + \mathrm{d}t$ using an Euler step: $\theta(\mathbf{r}, t + \mathrm{d}t) \simeq \theta(\mathbf{r}, t) + \mathrm{d}t\,(\partial\theta/\partial t)$.

A.2. Phase-Field program: dendritic growth using the model suggested by Kobayashi

See figure A1.

References

[1] Collins J B and Levine H 1985 *Phys. Rev.* B **31** 6119
[2] Kobayashi R 1993 *Physica* D **63** 410
[3] Karma A and Rappel W-J 1996 *Phys. Rev. Lett.* **77** 4050
[4] Kassner K and Misbah C 1999 *Europhys. Lett.* **46** 217
[5] Folch R, Casademunt J, Hernández-Machado A and Ramírez-Piscina L 1999 *Phys. Rev.* E **60** 1724
Folch R, Casademunt J, Hernández-Machado A and Ramírez-Piscina L 1999 *Phys. Rev.* E **60** 1734
[6] Borcia R and Bestehorn M 2003 *Phys. Rev.* E **67** 066307
[7] Biben T and Misbah C 2002 *Eur. Phys. J.* B **29** 311
[8] Biben T and Misbah C 2003 *Phys. Rev.* E **67** 031908
[9] Beaucourt J, Rioual F, Séon T, Biben T and Misbah C 2004 *Phys. Rev.* E **69** 011906
[10] Biben T, Misbah C, Leyrat A and Verdier C 2003 *Europhys. Lett.* **63** 623
[11] Roths T, Friedrich C, Marth M and Honerkamp J 2002 *Rheol. Acta* **41** 211
[12] Rowlinson J S and Widom B 1989 *Molecular Theory of Capillarity* (Oxford: Oxford University Press)